Assessment of Thermo-Osmosis Effect on Thermal Pressurization in Saturated Porous Media

Mohammadreza Mir Tamizdoust, S.M.ASCE[1]; and Omid Ghasemi-Fare, Ph.D., A.M.ASCE[2]

[1]Ph.D. Candidate, Dept. of Civil and Environmental Engineering, Univ. of Louisville, Louisville, KY. Email: m.mirtamizdoust@louisville.edu
[2]Assistant Professor, Dept. of Civil and Environmental Engineering, Univ. of Louisville, Louisville, KY. Email: omid.ghasemifare@louisville.edu

ABSTRACT

Coupled thermo-hydro-mechanical (THM) process in saturated porous media has been the subject of numerous studies. Recently, the influence of temperature gradient on the mass balance of fluid has been analyzed through the "thermo-osmosis effect" in low permeable soils, e.g., clay. In the case of thermal pore pressurization, the thermo-osmosis phenomenon causes the fluid flows away from the heat source and therefore alters the excess pore water pressure diffusion directly. Previous studies have shown that to better predict the thermal pressurization and thermal response of clayey soil, the thermo-osmosis phenomenon should be considered. Therefore, in the current study, a THM model with strong coupling is implemented in COMSOL multiphysics finite element software to assess the effect of thermo-osmotic flow in a saturated porous medium. The numerical results are compared with the experimental measurement of heating in Boom clay. The results show that thermo-osmotic flow leads to lower thermal pressurization in the vicinity of the heater; however, it does not affect the temperature distribution in the soil.

Keyword: Heat transfer; THM process; Thermo-osmosis; Thermal pressurization

INTRODUCTION

The analysis of thermo-hydro-mechanical (THM) behavior of low permeability soils is crucial when designing energy geo-structures, or deep geological reservoirs (Gens et al. 2007; Ghasemi-Fare and Basu 2016; Tamizdoust and Ghasemi-Fare 2019). In recent studies, the focus has been devoted to understanding the coupled THM process through the utilization of thermo-poromechanical constitutive models (Cui et al. 2000; Laloui and François 2009; Sultan et al. 2010) and thermo-mechanical macro and microstructure assessments (Abdelaziz et al. 2020; Joshaghani and Ghasemi-Fare 2019). In general, the temperature variation alters the hydraulic and mechanical aspects of soil media. One of the most important effects of thermal loadings in low permeable soils is the generation of excess pore water pressure, which is known as thermal pressurization, in undrained or weakly drained conditions due to the difference between the thermal expansion coefficients of saturating fluid and the pore volume (Ghabezloo and Sulem 2010; Zeinali and Abdelaziz 2020; Zeinali and Abdelaziz 2021). Moreover, Tamizdoust and Ghasemi-Fare (2020) showed that the thermo-poroelastic (TPE) constitutive model is successful in capturing the coupled THM process and thermal pressurization if temperature-dependent properties of the saturating fluid are accurately considered.

The coupled fluid flow in clays may also occur due to osmotic phenomena. In the presence of temperature gradient, the thermo-osmotic flow may greatly contribute to the mass transfer in

clays and directly influence the pore water pressure (Gonçalvès and Trémosa 2010; Trémosa et al. 2010). Gonçalvès et al. (2012) proposed the thermo-osmotic permeability coefficient based on physical molecular theory and incorporated it in a macroscale transport equation to investigate thermo-osmotic flow. Zagorščak et al. (2017) investigated the effect of thermo-osmotic flow with respect to thermal pressurization in Boom clay. More recently, Zhai and Atefi-Monfared (2020) presented a fully coupled analytical solution considering thermo-osmosis and thermal-filtration to study THM behavior of low permeability soils. It is to be noted that the temperature dependency of the thermal properties of the fluid was disregarded in these studies.

In the present study, a finite element analysis of thermal pressurization in Boom clay is investigated by considering the TPE constitutive model during a thermal loading in COMSOL Multiphysics. Furthermore, the thermo-osmotic flow is coupled with Darcy's flow to govern fluid flow due to hydraulic and thermal gradients. The results are compared with the in-situ measurements of the large-scale experiment called ATLAS in an underground research facility (HADES-URF) in Belgium (De Bruyn and Labat 2002).

THEORETICAL FORMULATION

The governing equations for THM modeling are stress equilibrium, mass balance (including Darcy and thermo-osmotic flow), and energy balance (Coussy 2004). All equations are formulated in Cartesian (x,y,z) coordinate system, where: $\partial(\bullet)/\partial t$, $\nabla(\bullet)$, $\nabla.(\bullet)$, and $\nabla^2(\bullet)$ are time derivate, gradient, divergence, and Laplace of field variables, respectively. Moreover, the Eulerian configuration of the continuum balance and constitutive equations with the assumption of small deformation is considered in this study.

Macroscopic Balance Equations

In this study, the saturating fluid is groundwater. The medium is consisting of incompressible solid particles with connected pores which is saturated with slightly compressible water. In addition, it is assumed that solid and fluid phases are in thermal equilibrium. Further, stress equilibrium is expressed as:

$$\nabla.\left(\boldsymbol{\sigma}' + p_f \mathbf{I}\right) + \left[n\rho_f + (1-n)\rho_s\right]\mathbf{g} = 0 \tag{1}$$

Total Cauchy stress, $\sigma = \sigma' + p_f \mathbf{I}$ (N/m^2), is decomposed to the Terzaghi's effective stress, σ' (N/m^2), and pore fluid pressure, p_f (N/m^2). $\mathbf{I}$ is the identity second-order tensor. It should be noted that the effective stress is related to the deformation of porous media through the non-linear elasticity model. In Equation (1), n (m^3/m^3), ρ_f (kg/m^3), and ρ_s (kg/m^3) are the porosity, water density, and solid density, respectively; and g (m/s^2) is the acceleration of gravity vector. The mass balances of solid skeleton and fluid (groundwater) are defined as:

$$\frac{\partial\left[(1-n)\rho_s\right]}{\partial t} + \nabla.\left[(1-n)\rho_s \mathbf{v_s}\right] = 0 \tag{2}$$

$$\frac{\partial\left(n\rho_f\right)}{\partial t} + \nabla.\left(n\rho_f \mathbf{q}\right) = 0 \tag{3}$$

where v_s (m/s) is the mass-averaged solid velocity vector, and q (m/s) is the fluid flux. In Equations (2) and (3) no mass exchange between solid and fluid phases are considered.

According to Gonçalvès et al. (2012), Darcy's and thermo-osmotic flow can be presented as follows:

$$n\mathbf{q} = -\frac{k}{\mu}\left(\nabla p_f + g\nabla z\right) - \frac{k_T}{\mu}\nabla T \tag{4}$$

In Equation (4), k (m^2) is the isotropic intrinsic permeability of the medium, μ (Pa.s) is the dynamic viscosity of the fluid, T (°C) is temperature and k_T ($Pa.m^2/°C$) is the thermo-osmotic permeability (k_T/μ is the thermo-osmotic conductivity).

The energy balance of the medium is defined as follows with respect to conduction and convection heat transfers:

$$\left(\rho C\right)_m \frac{\partial T}{\partial t} + \nabla.\left[n\rho_f C_f \mathbf{q} T - \lambda_m \nabla T\right] = 0 \tag{5}$$

In equation (5), $(\rho C)_m = n\rho_f C_f + (1-n)\rho_s C_s$ and $\lambda_m = n\lambda_f + (1-n)\lambda_s$, where, C_m, C_f, and C_s (J/kg/°C) are the specific heat capacity of the medium, water, and solid grains at constant stress, respectively. λ_m, λ_f, and λ_s (W/m/°C) are the thermal conductivity of the medium, water, and solid grains, respectively. Equations (1), (3), and (5) govern the solid stress, pore water pressure, and temperature fields.

To study fluid mass conservation considering the soil deformation and temperature variation, additional state variable equations are needed. Therefore, Equations (6) and (7) present the variations of the fluid density and the medium porosity with temperature, pore pressure, and effective stress. In Equation (7), the porosity change is governed by the linear thermo-poroelastic constitutive law where solid grains are assumed incompressible:

$$\frac{\partial \rho_f}{\partial t} = \rho_f \left(\left(\frac{1}{K_f} \right) \frac{\partial p_f}{\partial t} - \alpha_f \frac{\partial T}{\partial t} \right) \tag{6}$$

$$\frac{\partial n}{\partial t} = \left(1-n\right)\left[\frac{\partial \boldsymbol{\varepsilon}_{vol}^{e}}{\partial t} - \alpha_s \frac{\partial T}{\partial t} \right] \tag{7}$$

where K_f (1/Pa) and α_f (1/°C) are the bulk modulus and thermal expansion coefficient of Fluid, respectively. $\boldsymbol{\varepsilon}_{vol}^{e}$ (m/m) is the elastic volumetric strain, and α_s (1/°C) is the thermal expansion coefficient of solid grains. By incorporating Equations (6) and (7) in Equation (3), the fluid mass conservation equation is coupled with temperature and deformation fields.

According to the theory of elasticity, the increment of elastic strain is as follows:

$$d\boldsymbol{\varepsilon}^e = \mathbf{C}^e : d\boldsymbol{\sigma}' \tag{8}$$

where $\mathbb{C}^e$ (Pa) is the compliance elasticity 4th order tensor and is a function of Poisson's ratio, v (-) and Young's modulus, E (Pa), which is defined as (Modaressi and Laloui 1997):

$$E = E_{ref}\left(\frac{p'}{p'_{ref}}\right)^{m} \tag{9}$$

where E_{ref} (Pa) is the reference Young's modulus, p'=-I_1/3 is the mean effective stress, I_1 (Pa) is the first invariant of the stress tensor, p'_{ref} (Pa) is the reference pressure, and m (-) is a constant parameter.

Furthermore, previous studies by the authors (Joshaghani et al. 2018; Tamizdoust and Ghasemi-Fare 2020)indicate that the variations of α_f, μ, and λ_f are significant and cannot be ignored. Therefore, the thermodynamic properties of water are calculated based on the mathematical relations provided by the International Association for the Properties of Water and Steam (IAPWS) (Wagner and Kretzschmar 2008). Equations (10a)-(10c) present variations of the fluid properties with temperature.

$$\alpha_f = \left(0.00005T^3 - 0.01T^2 + 2T - 6\right)\times 10^{-5} \tag{10a}$$

$$\mu = \left(-0.0002T^3 + 0.05T^2 - 4T + 178\right)\times 10^{-5} \tag{10b}$$

$$\lambda_f = -0.000007T^2 + 0.0018T + 0.5711 \tag{10c}$$

Please note, the Equations (10a)-(10c) are valid for the temperature ranges from 0 to 100 °C.

In this study, the impact of temperature changes on pore fluid pressure due to variation of fluid's properties with temperature (e.g. dynamic viscosity and thermal expansion coefficient) and due to thermo-osmosis phenomenon is investigated. Despite the availability of many theoretical and numerical studies on THM analysis on soils, there are only a few studies that accurately consider the effect of temperature-dependent properties of the saturating fluid on the THM process in soil media (Braun et al. 2018; Ghabezloo and Sulem 2009). Therefore, an accurate numerical framework is needed to compare different aspects of temperature changes and mechanical deformation on THM behavior of clayey soils while thermo-osmosis phenomenon and real-time properties of soil and saturating fluid that are updated at each time step are considered.

DESCRIPTION OF NUMERICAL SIMULATION

ATLAS experiment

The theoretical model described in the previous section is used to simulate the thermal pressurization in Boom clay by considering thermo-osmosis flow. Boom clay is a natural overconsolidated deposit which is an appropriate porous environment for deep geological repositories in Belgium (François et al. 2009). Therefore, to validate the model, the ATLAS experiment is selected which was conducted in HADES underground research facility.

The ATLAS experiment consisted of a horizontal main borehole (19 m long) where the heater was located and two observation boreholes parallel to the main borehole (each 15.65 m long) where the measuring instrumentations were placed. The instrumentations measured the temperature, pore water pressure, and total stress variation. The observation boreholes were drilled at the distances of 1.184 m and 1.515 m away from the main borehole in the same horizontal plane. These boreholes were constructed perpendicular to the main gallery and in the

horizontal direction. Further, the experiment was conducted at the depth of 223m. The thermal loading associated with the ATLAS experiment during the first heating phase was equal to 900 W and lasted for 1075 days. The same level and duration of thermal loading are considered for the present numerical study. Moreover, the physical properties of Boom clay and material parameters used for the simulations are documented in the literature and are presented in Table 1 (Bernier et al. 2007).

Table 1. Physical Properties of Boom clay

Parameters	Values	Parameters	Values
ρ_{f0} **(kg/m^3)**	1000	λ_s (W/m/K)	1.65
ρ_s **(kg/m^3)**	2670	α_s (1/K)	1.3×10^{-5}
n_0 **(m^3/m^3)**	0.39	e_0 (m^3/m^3)	0.639
k_0 **(m^2)**	2.5×10^{-19}	υ (-)	0.125
K_f **(Pa)**	2.17×10^{9}	E_{ref} (Pa)	3.5×10^{8}
C_f **(J/kg/K)**	4200	m (-)	0.8
C_s **(J/kg/K)**	730	p_{ref} (Pa)	2.48×10^{6}

The governing balance equations and thermo-poroelastoplastic constitutive model are simultaneously solved in COMSOL Multiphysics v5.3a. A 2D axisymmetric horizontal domain (xy plane) is considered where the heat source is placed at the symmetry boundary. A rectangular domain geometry with 50 m in perpendicular (x-direction) and 69 m in parallel (y-direction) direction to the heat source is accounted to minimize the effect of boundary conditions on the results (Figure 1). The in-situ initial conditions of the experiment (z=223 m from the ground surface) are presented in Table 2 and are adopted in COMSOL. Constant temperature and pore water pressure equal to the initial values (Table 2) are considered for all boundaries except the axisymmetric one. After a series of mesh sensitivity analysis, the whole domain is discretized with 975 rectangular quadratic elements. Figure 1 presents the finite element meshes and a schematic view of the model. The set of PDEs presented in the previous section is implicitly solved using the PARADISO direct matrix solver which is available in the COMSOL Multiphysics software.

Table 2. The initial condition of the field variables

Parameters	Values
$\sigma_x = \sigma_y$ **(MPa)**	4.5
p_{f0} **(MPa)**	2.025
OCR	2.4
T_0 **(°C)**	16.5

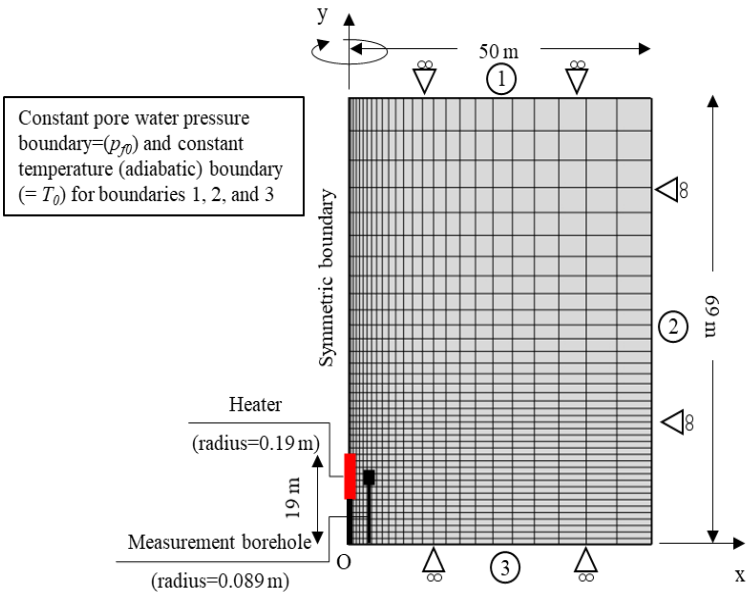

Figure 1. The numerical domain and boundary conditions

INTERPRETATION OF RESULTS AND DISCUSSION

The results of the numerical FE method are presented in this section. Two sets of numerical analyses with and without considering the thermo-osmosis phenomenon are compared. The value of thermo-osmotic conductivity (k_T/μ) is based on the model proposed by Gonçalvès et al. (2012), which was also used in Zagorščak et al. (2017). Thermo-osmotic conductivity is considered as a constant value for simplicity in this study (k_T/μ=3 $\times 10^{-12}$ $m^2/s/^oC$). Also, the effect of pressure gradient on heat flow also known as, the mechano-caloric effect is neglected. Figures 2 (a) and (b) show the variations of temperature and pore water pressure at a measurement borehole located at x=1.515 m from the heater. The simulated results are compared with the experimental observations. In Figure 2(a) the predicted result captures the behavior of the heat transfer in the vicinity of the heater with reasonable accuracy in comparison to the experiment. Moreover, the thermo-osmotic flow does not affect the heat transfer behavior of the soil. In general, the direct effect of thermo-osmotic flow on fluid diffusivity of the soil during the heating phase may increase the fluid flow; however, due to the very low intrinsic permeability of Boom clay, this effect is negligible on heat convection (Cherati and Ghasemi-Fare 2019; Ghasemi-Fare and Basu 2019). Figure 2(b) compares the effect of thermo-osmosis on thermal pressurization. As it can be seen from the figure, thermo-osmotic flow facilities the fluid diffusivity which means that thermally induced pore pressure is less pronounced in comparison to the results with no thermo-osmosis effect. It should be emphasized that in both cases thermal properties of water are considered as temperature-dependent variables though Equations 10 (a)-(c). Both types of numerical simulations underestimate the thermal pressurization during the heating phase.

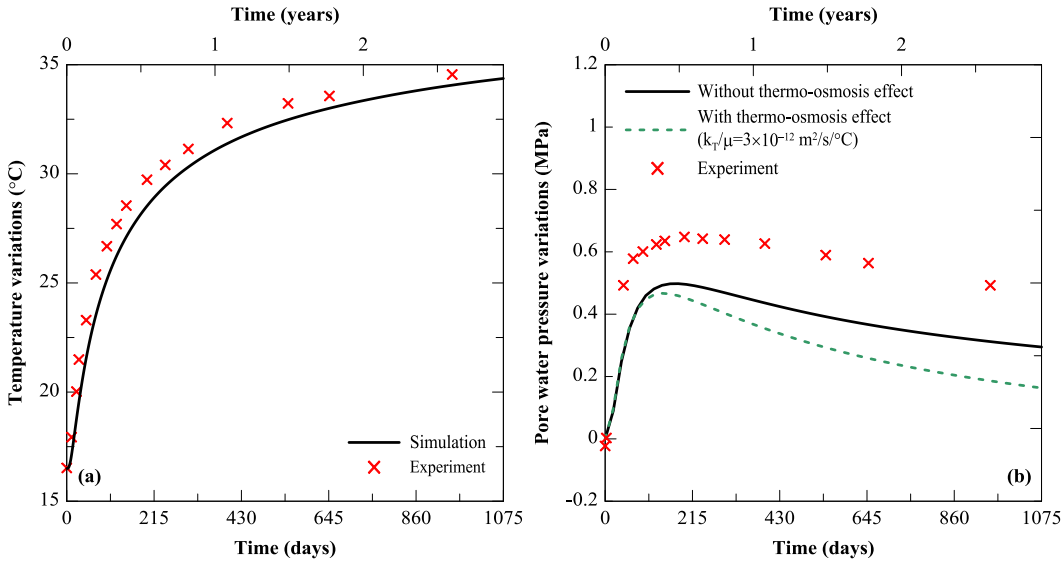

Figure 2. Comparison of (a) temperature, and (b) thermal pressurization variations with experimental observations at r=1.515 m from the heater

Figures 3 (a)-(c) illustrate the additional information about the thermo-hydro-mechanical process in the near field of the heater at different times of the heating phase. In Figure 3(a), the variations of temperature after 1 year of heating and at the end of the heating phase are shown. As mentioned before, the thermo-osmotic flow does not have a significant effect on soil thermal response (soil temperature); therefore, in this figure only the results obtained from a model that considers the thermo-osmosis phenomenon are presented. Figure 3(b) compares the effect of thermo-osmotic flow on thermal pressurization after 1 year of heating and at the end of the heating phase (3.5 years). As it can be seen in the figure, the thermal pressurization obtained from these two models is dissimilar. The difference in thermal pressurizations is higher close to the heater because of the higher thermal gradient. In addition, the results presented in Figure 3(b) depicts thermal pressurizations are varied for zones up to 7 m away from the heater at the end of the heating phase while it is 4 m after 1 year of heating since the influential zone of the temperature variation is smaller after 1 year of heating (See Figure 3a). Moreover, as it is expected thermo-osmosis flow increases the hydraulic diffusivity of the medium which leads to lower thermal pressurization. Figure 3(c) displays the mean effective stress variations because of the thermal loading and thermal pore pressurization. The decrease of the mean effective stress is due to thermal pressurization and expansive volumetric thermal strain. It is also observed that the reduction in mean effective stress is lower at the end of the heating phase due to the dissipation of the thermally induced pore water pressure. The results also confirm a lower reduction in mean effective stress close to the heat source when the thermo-osmotic flow is considered. This can be explained by lower thermal pressurization because of the pressure dissipation which was shown in Figure 3(b).

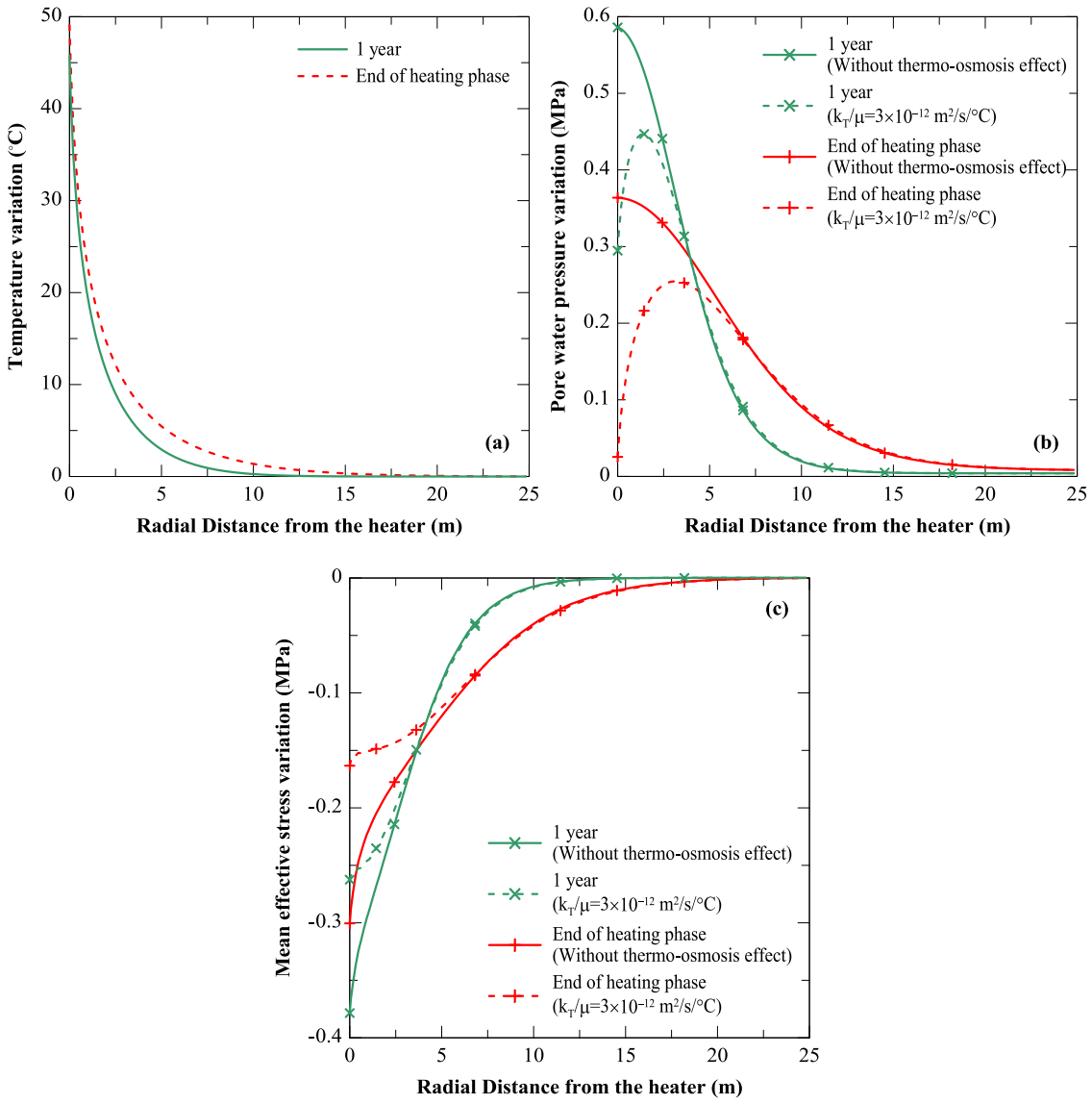

Figure 3. Variations of (a) temperature, (b) pore water pressure, and (c) mean effective stress along the radial distance from the heater for different times

CONCLUSION

In this study, a hydro-thermo-mechanical model is employed to investigate thermal pressurization with respect to thermo-osmotic flow as an addition to Darcy's flow. Experimental measurement on the thermal response of Boom clay in a deep geological repository is used to validate the numerical model. The effects of the thermo-osmosis phenomenon on temperature, pore pressure, and mean effective stress fields are compared. Thermo-osmotic flow facilitates the pore pressure diffusion which lowers the magnitude of thermal pressurization while has no significant effect on temperature variation. Lower thermal pressurization results in a lower change in mean effective stress close to a heat source when the thermo-osmotic flow is considered.

ACKNOWLEDGEMENT

The authors would also like to gratefully acknowledge the financial support from the National Science Foundation under Grant No. CMMI-1804822.

REFERENCES

Abdelaziz, S. L., Jaradat, K. A., and Zeinali, S. M. (2020). "Modified Thermomechanical Triaxial Cell for Microscopic Assessment of Clay Fabric Using Synchrotron X-Ray Diffraction." *Geotechnical Testing Journal*, 43(4).

Bernier, F., Li, X. L., and Bastiaens, W. (2007). "Twenty-five years' geotechnical observation and testing in the Tertiary Boom Clay formation." *Géotechnique*, 57(2), 229-237.

Braun, P., Ghabezloo, S., Delage, P., Sulem, J., and Conil, N. (2018). "Theoretical analysis of pore pressure diffusion in some basic rock mechanics experiments." *Rock Mechanics and Rock Engineering*, 51(5), 1361-1378.

Cherati, D. Y., and Ghasemi-Fare, O. J. G. (2019). "Analyzing transient heat and moisture transport surrounding a heat source in unsaturated porous media using the Green's function." 81, 224-234.

Coussy, O. (2004). *Poromechanics*, John Wiley & Sons.

Cui, Y. J., Sultan, N., and Delage, P. (2000). "A thermomechanical model for saturated clays." *Canadian Geotechnical Journal*, 37(3), 607-620.

De Bruyn, D., and Labat, S. (2002). "The second phase of ATLAS: the continuation of a running THM test in the HADES underground research facility at Mol." *Engineering Geology*, 64(2-3), 309-316.

François, B., Laloui, L., and Laurent, C. (2009). "Thermo-hydro-mechanical simulation of ATLAS in situ large scale test in Boom Clay." *Computers and Geotechnics*, 36(4), 626-640.

Gens, A., Vaunat, J., Garitte, B., and Wileveau, Y. (2007). "In situ behaviour of a stiff layered clay subject to thermal loading: observations and interpretation." *Géotechnique*, 57(2), 207-228.

Ghabezloo, S., and Sulem, J. (2009). "Stress dependent thermal pressurization of a fluid-saturated rock." *Rock Mechanics and Rock Engineering*, 42(1), 1.

Ghabezloo, S., and Sulem, J. (2010). "Temperature induced pore fluid pressurization in geomaterials." arXiv preprint arXiv:1011.6501.

Ghasemi-Fare, O., and Basu, P. (2016). "Thermally-induced pore pressure fluctuations around a geothermal pile in sand." *Geo-Chicago 2016*, 176-184.

Ghasemi-Fare, O., and Basu, P. (2019). "Coupling heat and buoyant fluid flow for thermal performance assessment of geothermal piles." *Computers Geotechnics*, 116, 103211.

Gonçalvès, J., de Marsily, G., and Tremosa, J. (2012). "Importance of thermo-osmosis for fluid flow and transport in clay formations hosting a nuclear waste repository." *Earth and Planetary Science Letters*, 339, 1-10.

Gonçalvès, J., and Trémosa, J. (2010). "Estimating thermo-osmotic coefficients in clay-rocks: I. Theoretical insights." *Journal of colloid and interface science*, 342(1), 166-174.

Joshaghani, M., and Ghasemi-Fare, O. (2019). "A Study on thermal consolidation of fine grained soils using modified triaxial cell." *Eighth International Conference on Case Histories in Geotechnical Engineering* ASCE, Philadelphia, Pennsylvania 148-156.

Joshaghani, M., Ghasemi-Fare, O., and Ghavami, M. (2018). "Experimental Investigation on the effects of temperature on physical properties of sandy soils." *IFCEE 2018*, 675-685.
Laloui, L., and François, B. (2009). "ACMEG-T: soil thermoplasticity model." *Journal of engineering mechanics*, 135(9), 932-944.
Modaressi, H., and Laloui, L. (1997). "A thermo-viscoplastic constitutive model for clays." *International journal for numerical and analytical methods in geomechanics*, 21(5), 313-335.
Sultan, N., Cui, Y.-J., and Delage, P. (2010). "Yielding and plastic behaviour of Boom clay." *Géotechnique*, 60(9), 657-666.
Tamizdoust, M. M., and Ghasemi-Fare, O. (2019). "Numerical Analysis on Feasibility of Thermally Induced Pore Fluid Flow in Saturated Soils." *Eighth International Conference on Case Histories in Geotechnical Engineering*, ASCE, Philadelphia, Pennsylvania, 73-82.
Tamizdoust, M. M., and Ghasemi-Fare, O. (2020). "A fully coupled thermo-poro-mechanical finite element analysis to predict the thermal pressurization and thermally induced pore fluid flow in soil media." *Computers and Geotechnics*, 117, 103250.
Tamizdoust, M. M., and Ghasemi-Fare, O. (2020). "Utilization of Non-equilibrium Phase Change Approach to Analyze the Non-isothermal Multiphase Flow in Shallow Subsurface Soils." *Water Resources Research*, e2020WR027381.
Trémosa, J., Gonçalvès, J., Matray, J., and Violette, S. (2010). "Estimating thermo-osmotic coefficients in clay-rocks: II. In situ experimental approach." *Journal of colloid and interface science*, 342(1), 175-184.
Wagner, W., and Kretzschmar, H.-J. (2008). "IAPWS industrial formulation 1997 for the thermodynamic properties of water and steam." *International Steam Tables: Properties of Water and Steam Based on the Industrial Formulation IAPWS-IF97*, 7-150.
Zagorščak, R., Sedighi, M., and Thomas, H. R. (2017). "Effects of thermo-osmosis on hydraulic behavior of saturated clays." *International Journal of Geomechanics*, 17(3), 04016068.
Zeinali, S. M., and Abdelaziz, S. L. "Effect of Heating Rate on Thermally Induced Pore Water Pressures and Volume Change of Saturated Soils." *Proc., Geo-Congress 2020: Geo-Systems, Sustainability, Geoenvironmental Engineering, and Unsaturated Soil Mechanics*, American Society of Civil Engineers Reston, VA, 31-39.
Zeinali, S. M., and Abdelaziz, S. L. (2021). "Thermal Consolidation Theory." *Journal of Geotechnical and Geoenvironmental Engineering*, 147(1), 04020147.
Zhai, X., and Atefi-Monfared, K. (2020). "Explanation of early failure in porous media confined with flexible layers, considering thermo-osmosis, thermal-filtration and heat sink from fluid dilation." *Computers and Geotechnics*, 122, 103501.